Continuous Navigation of an Inland Vessel with a Synthetic GNSS Antenna

Tobias Kersten, Le Ren, Steffen Schön

Leibniz Universität Hannover
Institut für Erdmessung
Hannover, GERMANY
Email: kersten@ife.uni-hannover.de

Abstract: *This paper describes a concept to obtain a continuous navigation and position solution of inland vessels based on a multi-GNSS antenna system. Also known as, "Virtual Receiver" we utilize this approach as an alternative method with respect to a common dead reckoning procedure.*

Such an approach strengthens the geometry of visible GNSS satellites immediatelyby up to 50%. At the same time, dilution of precision values improve by up to 40%. Hence, continuous navigation solution under difficult and challenging environmental conditions improves or is even possible. Specific experiments, obtained on a trip from Hannover westward on the Mittelland Canal with the inland vessel "MS Jenny" prove that various quality measures as well as the noise of the position estimates reduce significantly by up to 0.4 m. The position availability for code based navigation reaches 94.5% w.r.t classical single point positioning with 77%.

1. Introduction

Efficient and economic guidance of inland vessels relies on a continuouly, available, reliable and precise GNSS navigation solution. Hence, this is especially critical for passages beneath bridges or similar structures that cross the inland waterway. The freight transport on inland waterways is extreme reliable, almost safe and an effective possibility to transport freights of different kinds easily. The versatile loading reduces traffic stress from motorways [1]. Although, inland waterways provide an untapped potential for increasing inland waterway transport (ITW), Europe's market is stable since years at around 6.2% of total tonne-kilometres [2]. For ITW the fleet condition and infrastructure are bottlenecks nowadays. To ensure the safety and for providing assistance for collision warning and warnings of bridge clearance, robust and reliable GNSS based navigation solutions are required.

Currently, driver assistant concepts by means of GNSS rely on Real-Time Kinematic (RTK) approaches as described in [3], [4], [5], [6] and seems promising to assist the IWT with accuracies of decimetres to centimetres. However, to obtain such accuracy as well as precision, carrier phase based navigation is required. This is at least important for safety relevant applications. Discontinuities due to passages beneath bridges or other structures, show two effects: on the one hand, distortion (reflection, diffraction and interruption) of the incoming GNSS signals lead to complete loss-of-lock (LOL) of the carrier phases and code phase loops inside GNSS receivers. On the other hand, interruptions affect the ambiguity resolution. In addition, distortions of the signals are depending on the individual building structure of the bridge or infrastructure that crosses the canal.

In general, LOL are repaired using GNSS and couple it with external units, such as Inertial Navigation System (INS). However, alternatively combining more than one GNSS antenna and receiver units on a rigid platform is highly effective.

(a)

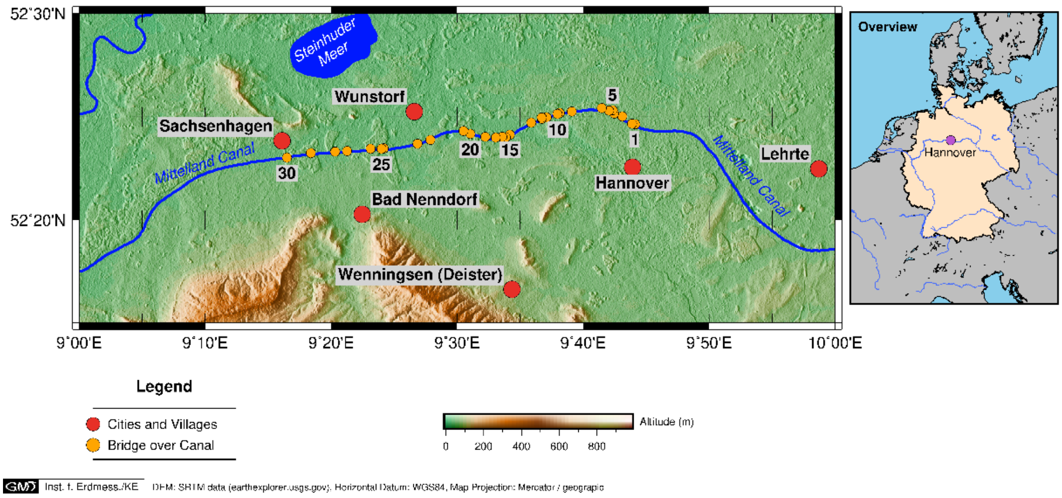

(b)

Figure 1: Inland vessel MS Jenny during kinematic scenario on June 27, 2016. Receivers are installed at the front (FRNT) and the rear (BACK) of the vessel (a), trajectory of investigated trip from Hannover westward to Minden on the Mittelland Canal as kinematic scenario (b).

This paper presents an alternate approach based on investigations by [7] [8] [9] [10] for continuous determination of position estimates to omit discontinuities or at least, to reduce them to a minimum. The approach combines a multi-antenna system as virtual receiver for the application on IWT without any utilisation of an INS.

The paper structure is as follows. In the next section, we describe the used navigation platform and the characteristics of available and recorded datasets. We discuss laboratory studies in the third section as the fourth section follows with detailed discussion of obtained results under real conditions for the code observables. Carrier phase observables are in focus in the fifth section. The paper finish with an outlook in the sixth and a summary in the seventh section.

2. The synthetic GNSS Antenna for Inland Waterway Transport

2.1 Specification of a synthetic GNSS antenna

The virtual receiver (VR) is a concept of combining observations from several antennas, distributed optimally on a rigid platform with known lever arm. The concept is implemented for and is used in the context of curved landing approaches of aircrafts. Nevertheless, it is applicable to arbitrary navigation platforms like, e.g. satellites, ferries or vessels. Hence, knowing the lever arm with required accuracy, the observations of several individual antennas are re-computable to a fixed location on the platform. This produces a *synthetic GNSS* *receiver antenna* that immediately provides an enlarged field of view w.r.t. individual antenna. This processing combines the observables in a *coordinated* manner. It improve the robustness of obtained position solution easily; improve the satellite visibility, position availability and various dilution of precision (DOP) values. Several applications prove that this approach can guaranty continuous navigation solutions. This is of special interest for safety-relevant flight approaches as shown in [8] [9] [11]. In combination with precise point positioning (PPP) this approach leads to improved reliability, continuity and precision for low earth orbiters (LEO) [10]. Marine applications are firstly demonstrated by [12] for a ferry in the Galileo SEAGATE test environment in Rostock, Germany.

In general, the lever arm requires additional attitude angles to consider the transport rate. Furthermore, the individual receiver require a synchronization. Thus, the overall quality of the VR solution is at least depending on the lever arm, the attitude angles and the individual receiver/antenna equipment.

2.2 Mathematical model of the virtual receiver

Since we fixed for our studies the VR in the FRNT location, Eq. (1) shows the rough mathematical concept for a code based position solution for the virtual receiver. The code observation equation P_B^k at the location BACK to a k^{th} satellite forms to

$$P_B^k = \sqrt{(X^k - (x_{vr} - \Delta x))^2 + (Y^k - (y_{vr} - \Delta y))^2 + (Z^k - (z_{vr} - \Delta z))^2} + \partial t_B + \varepsilon \qquad (1)$$

with the Earth Centred Earth Fixed (ECEF) coordinates of the satellite $[\vec{X}^k]$, the position of the VR $[\vec{x}_{vr}]$, the lever arm $[\Delta\vec{x}]$, the receiver clock estimate ∂t_B and the accumulation of remaining errors like, e.g. satellite clock, ionosphere etc. in ε. Consequently, the equation for the FRNT location P_F^k including the individual receiver clock estimate ∂t_F reads

$$P_F^k \sqrt{(X^k - x_{vr})^2 + (Y^k - y_{vr})^2 + (Z^k - z_{vr})^2} + \partial t_F + \varepsilon \qquad (2)$$

Which results in the design matrix A for an epoch wise least-squares adjustment (LSA). Here we have a number of five unknowns, as the individual receiver clock estimate of each involved receiver antenna has to be considered in addition. This results in

$$A = \begin{bmatrix} \frac{\partial P_B^1}{\partial x_{vr}} & \frac{\partial P_B^1}{\partial y_{vr}} & \frac{\partial P_B^1}{\partial z_{vr}} & 1 & 0 \\ \vdots & \vdots & \vdots & \vdots & \vdots \\ \frac{\partial P_B^k}{\partial x_{vr}} & \frac{\partial P_B^k}{\partial y_{vr}} & \frac{\partial P_B^k}{\partial z_{vr}} & 1 & 0 \\ \cdots & \cdots & \cdots & \cdots & \cdots \\ \frac{\partial P_F^1}{\partial x_{vr}} & \frac{\partial P_F^1}{\partial y_{vr}} & \frac{\partial P_F^1}{\partial z_{vr}} & 0 & 1 \\ \vdots & \vdots & \vdots & \vdots & \vdots \\ \frac{\partial P_F^k}{\partial x_{vr}} & \frac{\partial P_F^k}{\partial y_{vr}} & \frac{\partial P_F^k}{\partial z_{vr}} & 0 & 1 \end{bmatrix} \qquad (3)$$

3. Dedicated Studies on Inland Waterway Transport

3.1. The navigation platform: the inland vessel *MS Jenny*

Since 2002 and on behalf of the Federal Ministry of Education and Research, the motor freight ship *MS Jenny* (MS Science) annually travels as a *swimming science centre* with changing topics of exhibitions on inland waterways through Germany.

The dimensions of the vessel are: 100 m length, 9.5 m width and 3.16 m depth. For the general navigation, a Radarpilot 720° unit is available. The vessel provides optimal conditions to utilize it as a mobile GNSS platform. Our group was pleased to have the opportunity to use this optimal environment.

3.2 Datasets for laboratory studies

In June 2016 and 2018 we recorded several datasets. The investigations presented in this paper will focus on campaigns from June 27, 2016 (DOY179). Here, we study two data records in more detail. The first record origins from the time, as the vessel laid at the mooring point in Hannover, assigned in this paper as *semi-kinematic scenario* (DOY179-1). The second record is a trip from Hannover westward on the Mittelland Canal with a duration of a 2.5 hours. This dataset is a *kinematic scenario* (DOY179-2). Ref. [13] discusses the obtained results in more detail. During the kinematic scenario, the vessel passed beneath 30 bridges and infrastructures as shown in Fig. 1(b).

3.3 Hardware set-up

Instruments Two different GNSS receiver types are in use to investigate their individual behaviour on the discontinuities of bridge passing and appearing interruptions. We have had the opportunity to set up two GNSS receivers on the inland vessel MS Jenny. Fig. 1(a) indicates both mountings by circles. At the front (FRNT), we installed a Javad Delta TRE_G3T receiver and a Novatel NOV703GGG.R2. At the rear (BACK), a Novatel SPAN-SE is in use with the same receiver antenna type as setup for FRNT.

Lever arm The lever arm between FRNT and BACK was obtained by RTK and tachymeter during the time, the ship laid at the mooring point. A distance of 57.34 m with standard deviation of 2 cm was determined.

Reference Trajectory The reference trajectory for the *semi-kinematic scenario* (DOY179-1) is provided by carrier phase based double difference (DD) processing using Novatel GrafNav Software (Vers. 8.50.4923) with individual antenna phase centre corrections (PCC) and precise products from the centre of orbit determination in Europe (CODE) [14]. For the DD computations, we used the reference station at our GNSS laboratory in Hannover. Additionally, we process trajectories using the online PPP service like, e.g. NRCan [15]. Thus, we processed the reference trajectory for the *kinematic scenario* (DOY179-2) correspondingly. However, as bridge passages invoke mostly complete loss-of-lock (LOL) on the carrier phase observation, an enhanced ambiguity fixing is required to bridge the misleading ambiguity resolution between bridges. Ref. [3] and [16] discuss similar requirements for RTK.

Specification for Inland Waterway Transport GNSS signal interruptions differ between vessels and airplane or satellite applications. Hence, based on the ship geometry and other conditions, which lead to LOL and signal interruptions, we used bow and stern of the ship to provide a maximum distance between both individual antenna locations (cf. Fig. 1(a)). Since the vessel travels with a mean velocity of 10-12 km/h, at least one antenna provides enough GNSS observables to bridge passages where individual antennas will have signal interruptions, but the *synthetic GNSS antenna* will not.

3.4 Processing strategy

We processed a single point positioning for the FRNT location (SA) and compare this solution with the VR. Therefore, we fix the VR and re-compute the observables to the FRNT location with the information of the lever arm. During the computation, we utilized our in-house developed software. As indicated by Table 1, different weighting schemes are applied. On the one hand, identical weighting (IDEN) and on the other hand, elevation dependent weighting (COS2). A cut-off angle of 2° applies for both, the *semi-kinematic* and the *kinematic scenario*. Studies on the carrier phase for GPS L1 DD are computed utilizing a moving baseline and using our own software, too.

4. Results of Code Processing

4.1 Satellite visibility

Fig. 2(a) summarises the satellite visibility for the semi-kinematic scenario at the mooring point. During this approximate one hour, the satellite visibility is improved by more than 54%. For the SA case a mean number of only eight satellites was visible whereby at the same time, the synthetic GNSS antenna with the VR approach has an amount of 17.3 satellites in view. Similar findings are present for the kinematic scenario. Here, during the whole trip, a mean number of 9.3 satellites were visible in the SA but 17.1 for the VR case (cf. Fig. 2(b)).

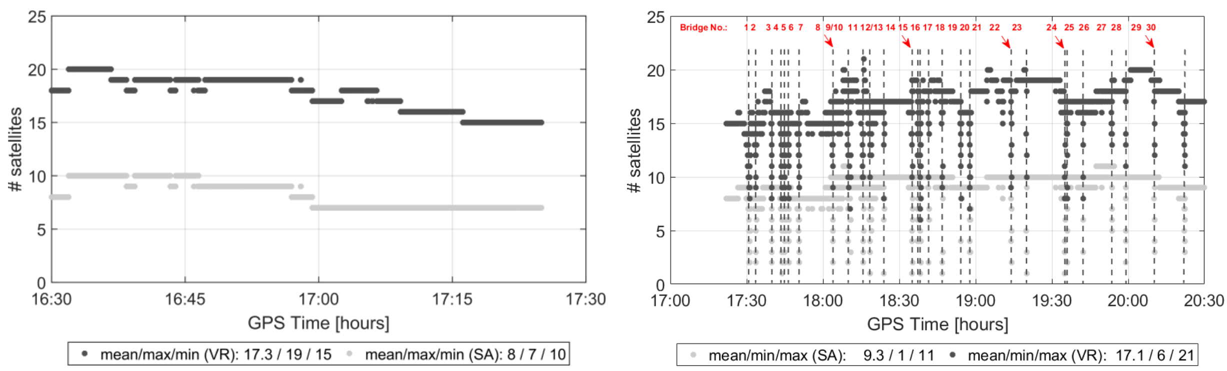

(a) (b)

Figure 2: Number of visible satellites. Cases of SA and VR shown for both scenarios, semi-kinematic (a) and kinematic scenario (b). During the trip between Hannover westward on the Mittelland Canal, 30 bridges are passed and assigned by gray dashed lines including the individual bridge number in (b).

4.2 Dilution of precision

The accuracy of range measurements is limited by various errors like e.g., signal propagation in the atmosphere, at the GNSS receiver and antenna as well as due to the entire surrounding at each individual GNSS receiver antenna. Therefore, errors on the position domain results from the errors on the range measurement multiplied by a factor of geometry, the dilution of precision (DOP) values **[17]** **[18]**. Fig. 3 depicts several subsects of the geometric DOP (GDOP). It shows that a synthetic GNSS antenna with the VR approach is extremely advantageous to strengthens the satellite geometry and to provide a significant reduction of expectable DOP values. As indicated by Fig. 3(a), the accuracy of the position improves by about 40% for the scenario at the mooring point. Focussing on the topocentric subsects like e.g., the horizontal DOP (HDOP) and the vertical DOP (VDOP) we summarize that the improvements are higher in the case of VDOP than in the case of HDOP. This is especially true for the time around 17:00 where the constellation of visible satellites changed in the SA case but is stable in the VR case. There, improvements in the VDOP of up to 1.1 are noticeable, for HDOP they are around 0.7-0.8.

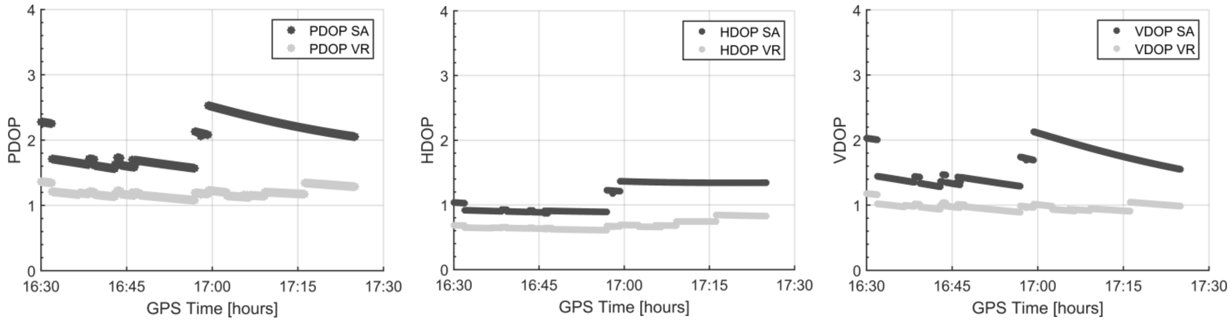

(a) (b) (c)

Figure 3: Various subsects of dilution of precision values (DOP) for the semi-kinematic scenario at the mooring point in Hannover; subplots show the position DOP (PDOP) (a), horizontal DOP (HDOP) (b) and vertical DOP (VDOP) (c).

4.3 Accuracy and position availability

The position error (PE) w.r.t. a reference trajectory reflects a measure of accuracy and is computed by

$$\Delta\hat{\boldsymbol{x}} = \hat{\boldsymbol{x}} - \boldsymbol{x} \tag{4}$$

with $\hat{\boldsymbol{x}}$ being the reference trajectory and $\boldsymbol{x}$ the corresponding SA or VR solution. In a local topocentric system, the accuracy measures are separated into a horizontal position error (HPE)

$$\text{HPE} = \sqrt{(\Delta\boldsymbol{x}_N^2 + \Delta\boldsymbol{x}_E^2)} \tag{5}$$

and a vertical position error (VPE), which reads

$$\text{VPE} = |\Delta\boldsymbol{x}_U| \tag{6}$$

For both scenarios, we summarized the processed solutions in Table 1 for different weightings.

Focussing on the first scenario at the mooring point, the VR completely outperforms the SA results. However, the availability of position is quite similar, since at none of the individual antennas LOL are present. Nevertheless, this changes, when focussing on the results from Tab. 1 in the case of the second scenario. Here, passages of bridges and similar structures above the canal lead to LOL at individual antennas. In the case of using the synthetic GNSS receiver antenna and the VR approach, these interruptions could be repaired and result in more consistent position availability and improved HPE and VPE.

In addition, Fig. 4. shows the subsects of the topocentric deviations w.r.t. the reference solution of the first scenario in Hannover. As shown, the noise on all three components reduce by more than 0.4 m due to strengthened geometry by the synthetic GNSS receiver antenna. These results coincide well to the findings of the semi-kinematic scenario presented in Tab. 1.

Table 1: Comparisons of several processing strategies on the performance of VR and SA for semi-kinematic and kinematic sessions.

		VR		**SA**	
		IDEN	**COS2**	**IDEN**	**COS2**
semi-kinematic scenario (DOY179-1)	HPE [m]	0.92	0.70	1.35	1.02
	VPE [m]	0.68	0.46	0.90	0.54
	Availability [%]	**100**	**100**	**99.8**	**99.9**
kinematic scenario (DOY179-2)	HPE [m]	0.76	0.68	1.03	0.97
	VPE [m]	0.49	0.48	0.78	0.71
	Availability [%]	**93.7**	**94.5**	**80.3**	**76.7**

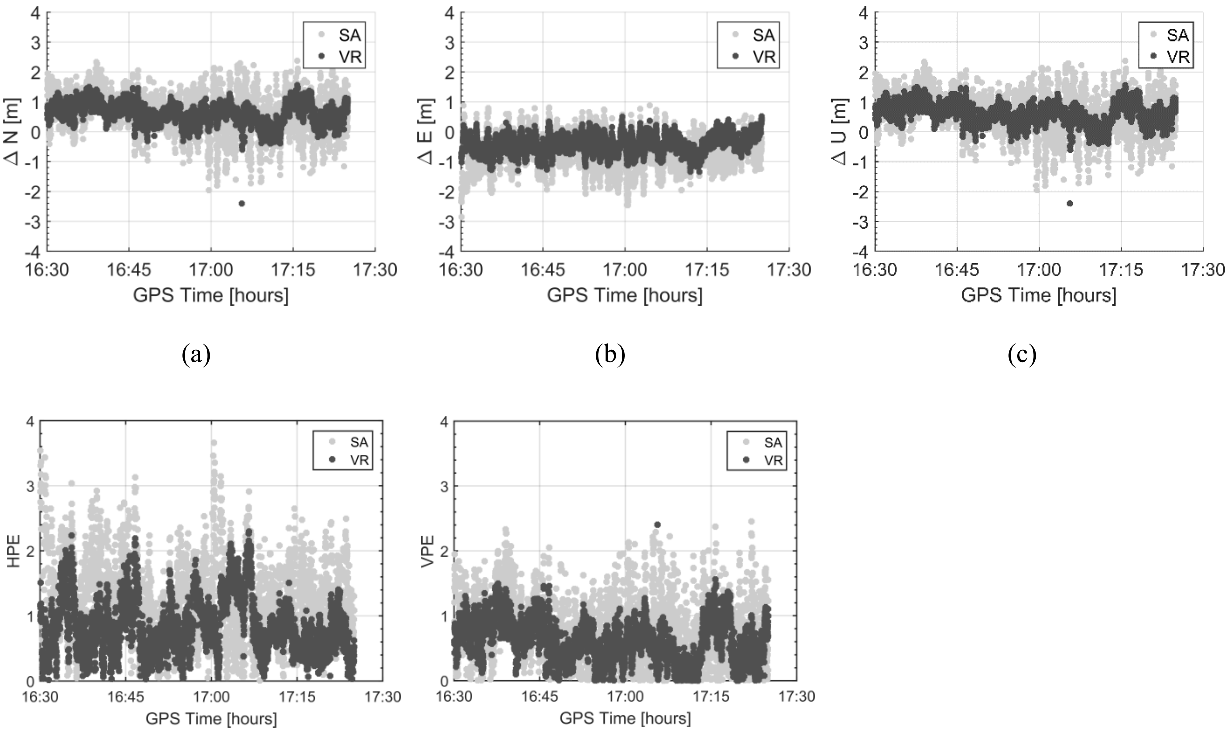

(a) (b) (c)

(d) (e)

Figure 4: Time series of position deviations from reference position in local topocentric system for the semi-kinematic scenario at the mooring point; north component (a), east component (b) and up component (c) as well as position errors (PE) in terms of topocentric components, horizontal PE (HPE) (d), vertical PE (VPE) (e) for IDEN processing.

5. Results of Carrier Phase Processing

5.1 Station specific characteristics

To investigate the impact of the ship on the electromagnetic GNSS signal and furthermore the passages of bridges, we study the baseline between bow and stern of the vessel w.r.t. the carrier phase signal of GPS on the frequency L1. Therefore, we utilize the approach of a moving baseline, which means we process a relative solution between two moving receiver antennas and fixed relative distance. The geometry of the lever arm introduces the information for the relative fix. In correspondence to the Sec. 4, the base of the moving baseline is set at the FRNT location.

Since different, individual receiver were in use, we summarize their individual quality parameters in Fig. 5 for the code and carrier phases at both locations for the semi-kinematic scenario. Both locations provide close similar satellite visibilities w.r.t. the ship axis. However, taking a closer look into the multipath linear combination (MP) [19], [20] which we calculate for the frequency GPS L1 using RINEX3 [21] observations types GC1C, GL1C and GL2W, different characteristics are noticeable (cf. Fig 5(b) and Fig 5(e)). The FRNT provides unsmoothed carrier phase observables, as the BACK uses a default code-/carrier smoothing. In general, vessels have challenging reception conditions w.r.t. the antenna characteristics due to materials with high dielectric constants in close vicinity. Moderate code multipath is detectable at both locations, whereby the smoothing at BACK leads to some magnitudes with less noise than expected at FRNT. The higher magnitudes at BACK are in correspondence with actions on the vessel at the mooring point at this time, as several preparations for the departure were running. The signal-to-noise (C/N0) time series are quite comparable and show typical structures at least for ascending and descending satellites. This gets more challenging for the carrier phase observable, when signal interruptions due to bridge passages occur. Signal characteristic w.r.t. IWT are discussed in [13] in detail, therefore.

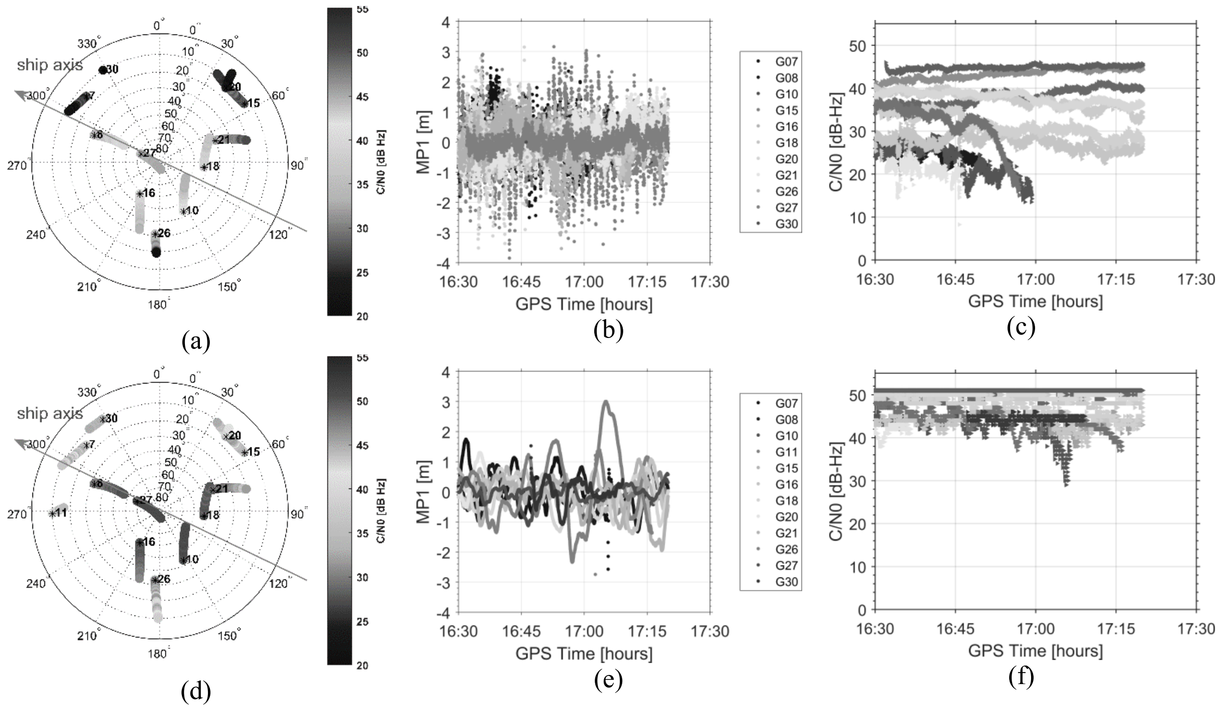

Figure 5: Station characteristics of FRNT (a-c) and BACK (d-f) receiver antenna location, with the following columns: Skyplot with ship axis w.r.t. topocentric system (1), multipath MP1 (GC1C, GL1C, GL2W) linear combination (2), C/N0 for individual satellites over time (3).

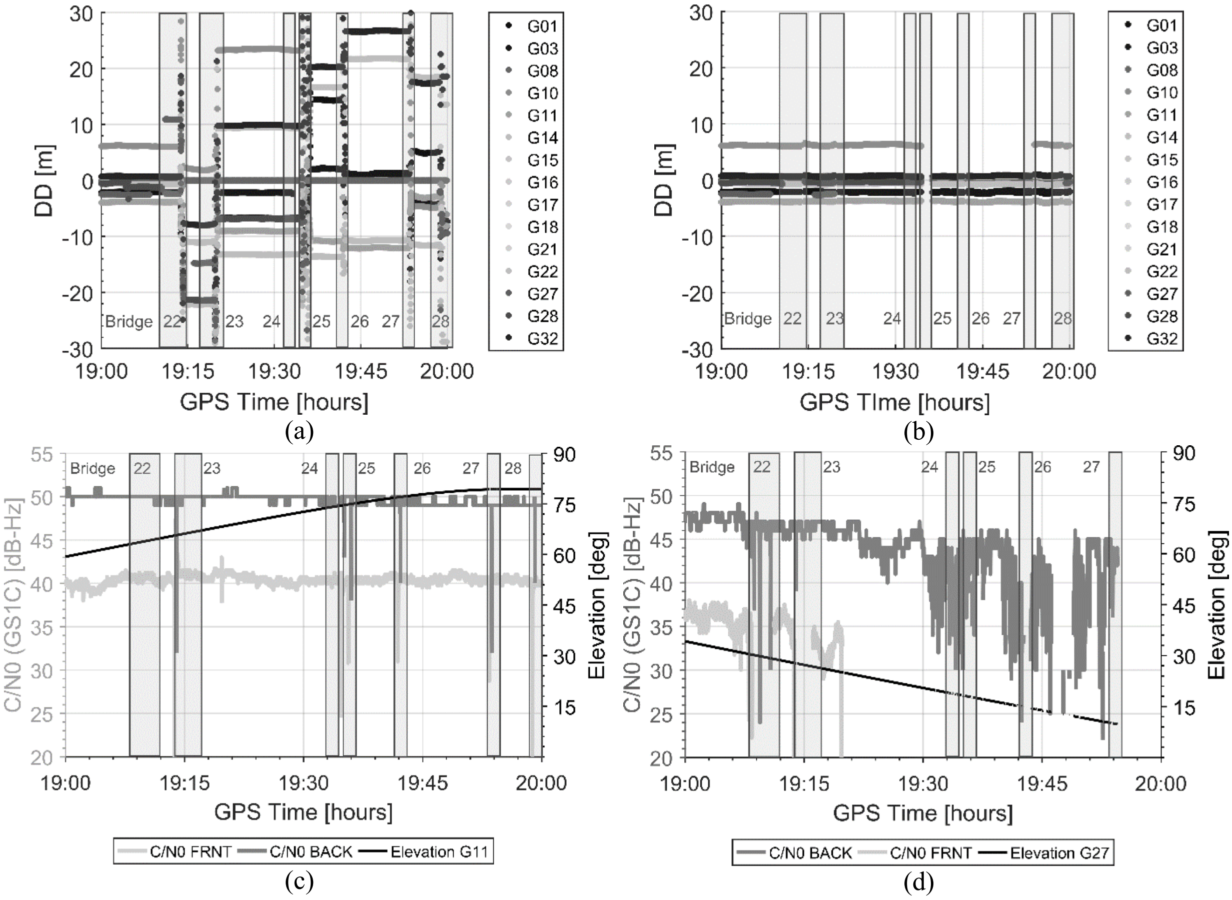

Figure 6: Details for the baseline between FRNT and BACK during kinematic scenario with indicated bridges; GPS L1 carrier phase double differences (DD) with interruptions (a), repaired DD (b), C/N0 of ascending GPS satellite G11 w.r.t. direction of travel (c) and for G27 descending w.r.t. direction of travel (d).

5.2 Baseline processing and analysis

Fig. 6 collects several details to show the difficulties for the carrier phase based navigation in IWT and vessel navigation. As discussed in Sec. 4, passages due to infrastructures above the canal, like e.g., bridges, barrage gates etc., lead to entire LOL on the carrier, code phase observables, and impose difficulties in the ambiguity resolution. This is especially critical for safety relevant applications in (near-) real-time. Fig. 6(a) indicates that signal distortions are clearly detectable with sudden signal distortions and losses. Thus, magnitudes of several decimetres of the GPS L1 carrier phase double difference observable result. Although, carrier phase observations are available after the passages of infrastructures, their ambiguity value differ after each passage significantly and systematically. Furthermore, in cases where bridges or LOL occur closely to each other, an ambiguity resolution is not possible or the convergence time cannot be reached. This is true for both, a baseline solution computed based on individual PPP solutions for FRNT and BACK, which we obtained by online PPP services and GravNav processing, and for a processing of a moving baseline without enhanced cycle slip detection. Clean DD for a moving baseline are obtainable when utilising a post processing with enhanced cycle slip detection and correction mechanism. In general, the C/N0 could be an important indicator to detect signal interruptions in real-time applications. Therefore, Fig. 6(c) collects C/N0 of both, FRNT and BACK, for the time of the kinematic scenario w.r.t. an rising satellite (GPS G11) of good visibility. In addition, Fig 6(d) summarises the corresponding observables for a setting satellite (GPS G27) of challenging visibility. Sudden jumps of the C/N0 and the corresponding DD due to bridges (exemplarily shown for bridge number 22-28) are detectable. Tab. 2 summarises the corresponding individual building structures. First studies with 10 Hz data recording intervals indicate that individual building structure could be identified by individual characteristics w.r.t. the signal interruptions and distortions. However, the proposed approach of a synthetic GNSS antenna with the concept of a VR could be used to bridge and repair carrier phase ambiguities since the geometry between the antennas by the lever arm is known. The re-computed observables from individual receiver antennas into a unique VR solution could assist the ambiguity resolution. In addition, our obtained results of a kinematic baseline on a vessel show the expected noise (cf. Fig. 5(b,e)) although the general construction of a vessel provides many materials of high dielectric constants which surround the individual GNSS receiver antennas. Hence, the noise of the obtained DD solution for the moving baseline results into a deviation of ±2 cm with systematic oscillations of up to ±5 cm.

Table 2: Bridge characteristics for studied time of the kinematic scenario between the time 19:00-20:00 o'clock.

Bridge	**Function**	**Lanes**	**Building Structure**	**Time of arrival (@FRNT)**	**Width**	**Distance under bridge**
				[hours]	[m]	[m]
22	car	2	Flat	19:14	15	15
23	farm lane	1	Flat	19:19	8	8
24	railway	2	metal arc	19:35	13	17
25	car	2	flat	19:35	13	14
26	pedestrian	1	metal arc	19:42	6	6
27	car	2	metal arc	19:53	8	8
28	car	1	metal arc	19:59	5	5

6. Future Aspects and Further Projects

For the future work, there are several items open, which will be investigated by our group in future. Therefore, a consistent combination of methods and improved hardware set-ups in the sense of a multi-system unit (RTK-approach, antenna, infrastructure, navigation processing) will be in focus.

The instruments and in special, here the GNSS antennas can be a bottleneck. Hence, new multipath mitigation techniques are available especially for RTK approaches. In cf. [22] very promising results are shown to improve the overall GNSS observation quality in the sense of multipath in such a multi-sensor-system.

For the infrastructure, a mass-market RTK service is required. At present, here are several distributors with different services available. However, a comprehensive infrastructure on inland canals is not exiting yet. Focussing on mass-market products, several companies and joint ventures pointing explicitly on those key questions. As for the majority, their infrastructure is mainly managing the autonomous driving sector; this will assist a comprehensive network infrastructure for assisted and autonomous inland vessel navigation, additionally.

Further investigations look promising to benefit from the VR approach, which is the application of receiver clock modelling [23], as the geometry and therefore the stability of the satellite visibility improves, [24]. This approach will be additionally beneficial for navigation under challenging conditions. For several navigation scenarios, it could be demonstrated, that the most benefit for the receiver clock modelling is to find for the up component. This component is at present the most challenging component, at least for the height detection of bridges, which are passed by inland vessels.

7. Conclusion

This paper shows a concept of forming a synthetic GNSS receiver antenna by combining measurements of individual antennas with known lever arm. Using the concept of a virtual receiver improves both, the navigation geometry w.r.t. visible satellites and the position accuracy and availability.

We applied the concept to IWT using a vessel and could demonstrate promising results. The satellite visibility improves by up to 50%, which leads to significant lower DOP values of up to 40% for both, the semi-kinematic and the kinematic scenario. Focussing on the bridge passages, where signal interruptions lead to challenging and difficult situations for positioning, the position availability w.r.t. a classical SA solution improves by 13-16%, depending on the weighting scheme. However, the position availability in the kinematic case changes from 76.7% in the case of SA to 94.5% in the case of VR.

The enhanced observation continuity driven by the synthetic GNSS antenna looks promising to avoid faults of the carrier phase ambiguity resolution that are caused by LOL and entire signal distortions at individual antenna locations in close vicinity to bridge passages.

Acknowledgement

The investigations of this project were driven by a one-year student project seminar on the topic of Navigation and Positioning at the Leibniz University Hannover. Therefore, the authors like to thank in addition all the contributors for this valuable project, namely Lucy Icking, Sara Brakemeier, Arman Kharma, Fabian Ruwisch and Vahid Aghajani.

Furthermore, we like to acknowledge the Center of Orbit Determination in Europe for providing precise orbit and satellite products.

At least, very special and warm thanks the first author would like to dedicate to the captain family of the MS Jenny (MS Wissenschaft) Fam. Scheubner for their grateful support and interest on this project and their familiar hosting during the GNSS campaigns.

References

[1] W. Sihn, H. Pascher, K. Ott, S. Stein, A. Schumacher and G. Mascolo, "A Green and Economic Future of Inland Waterway Shipping," *Procedia CIRP,* vol. 29, pp. 317-322, 2015.

[2] Eurostat, "Modal split of freight transport in Europe," 2018.

[3] M. Hoppe, "GNSS-Anwendungen in der Schiffahrt," vol. 87, pp. 93-105, 2 2017.

[4] A. Hesselbarth, R. Zeibold, M. Sandler, J. Alberding, M. Uhlemann, M. Hoppe, M. Bröschel and L. Burmisova, "Towards a Reliable Bridge Collision Warning System for Inland Vessel Navigation Based on RTK Height Determination," in *Proceedings of the 30th International Technical Meeting of The Satellite Division of the Institute of Navigation (ION GNSS+ 2017)*, 2017.

[5] L. Wanninger, "Virtuelle GPS-Referenzstationen für großräumige kinematische Anwendungen," *ZfV,* vol. 128, pp. 196-202, 2003.

[6] D. Medina, A. Hesselbarth, R. Büscher, R. Ziebold and J. García, "On the Kalman Filtering Formulation for RTK Joint Positioning and Attitude Quaternion Determination," in *IEEE/ION PLANS 2018*, 2018.

[7] S. Nair and C. Bartone, “Multiple antenna GPS configuration for enhanced performance,” *Proceedings of ION AM, Institute of Navigation, June 7-9, Dayton, Ohio, USA,* pp. 188-199, 2004.

[8] F. Kube, S. Schön and T. Feuerle, “Virtual receiver to enhance GNSS-based curved landing approaches,” *Proceedings of ION GNSS 2011, Portland, Oregon, USA,* pp. 536-545, 2011.

[9] F. Kube, S. Schön and T. Feuerle, “GNSS-based curved landing approaches with a virtual receiver,” in *ION PLANS*, 2012.

[10] F. Kube, C. Bischof, P. Alpers, C. Wallat and S. Schön, “A virtual receiver concept and its application to curved aircraft-landing procedures and advanced LEO positioning,” *GPS Solutions,* vol. 22, p. 41, 13 2 2018.

[11] F. Kube, S. Schon and T. Feuerle, “Improved navigation performance for curved approaches with a virtual receiver,” in *2012 6th ESA Workshop on Satellite Navigation Technologies (Navitec 2012) & European Workshop on {GNSS} Signals and Signal Processing*, 2012.

[12] S. Schön and P. Alpers, “A Virtual receiver for Pseudolites: Enhancing the positioning and Heading Determination of a Ferry,” in *Proc ION GNSS+ Miami Florida, 24.-26.9.2018*, 2018.

[13] T. Kersten, L. Ren and S. Schön, “A Virtual Receiver Concept for Continuous GNSS based Navigation of Inland Vessels,” in *Navitec 2018, December 5-7, Noordwijk, The Netherlands*, 2018.

[14] R. Dach, S. Schaer, D. Arnold, L. Prange, D. Sidorov, P. Stebler, A. Villiger and A. Jäggi, “CODE final product series for the IGS,” *Published by Astronomical Institute, University of Bern,* 2018.

[15] T. Nylen and S. White, “Online Precise Point Positioning Using the Natural Resources Canada Canadian Spartial Reference System (CSRS-PPP),” *UNAVCO,* p. 8, 2007.

[16] A. Hesselbarth, “GNSS in der Hydrographie,” in *170. DVW-Seminar und 32. Hydrographentag*, 2018.

[17] P. Massat and K. Rudnick, “Geometric Formulas for Dilution of Precision Calculations,” *Navigation,* vol. 37, pp. 379-391, 1990.

[18] R. Santerre, A. Geiger and S. Banville, “Geomtery of GPS Dilution of precision: revisited,” *GPS Solution,* vol. 21, pp. 1747-1763, 2017.

[19] S. Hilla and M. Cline, “Evaluating pseudorange multipath effects at stations in the National CORS Network,” *GPS Solutions,* vol. 7, pp. 253-267, 3 2004.

[20] A. Bilich and K. M. Larson, “Mapping the GPS multipath environment using the signal-to-noise ratio (SNR),” *Radio Science,* vol. 42, 11 2007.

[21] W. Gurtner and L. Estey, “RINEX - The Receiver Independent Exchange Format,” *International GNSS Service (IGS), RINEX Working Group and Radio Technical Commission for Maritime Services Special Committee 104 (RTCM-SC104),* 2015.

[22] D. V. Tatatarnikov, A. P. Stephanenko and A. V. Astakhov, “Moderately compact helix antennas with cutoff patterns for millimeter RTK positioning,” *GPS Solution,* vol. 20, pp. 587-594, 4 2016.

[23] T. Krawinkel and S. Schön, “Benefits of receiver clock modeling in code-based GNSS navigation,” *GPS Solutions,* vol. 20, pp. 687-701, 8 2015.

[24] R. Santerre and A. G. Simon Banville, “Geomtery of GPS Dilution of precision: revisited,” *GPS Solution,* vol. 21, pp. 1747-1763, 2017.